

Practical Evaluation of Adversarial Robustness via Adaptive Auto Attack

Ye Liu¹, Yaya Cheng¹, Lianli Gao¹, Xianglong Liu², Qilong Zhang¹, Jingkuan Song^{1*}

¹ Center for Future Media and School of Computer Science and Engineering
University of Electronic Science and Technology of China, China

² Beihang University, China

liuye66a@gmail.com, yaya.cheng@hotmail.com, lianli.gao@uestc.edu.cn
xlliu@buaa.edu.cn, qilong.zhang@std.uestc.edu.cn, jingkuan.song@gmail.com

Abstract

Defense models against adversarial attacks have grown significantly, but the lack of practical evaluation methods has hindered progress. Evaluation can be defined as looking for defense models' lower bound of robustness given a budget number of iterations and a test dataset. A practical evaluation method should be convenient (i.e., parameter-free), efficient (i.e., fewer iterations) and reliable (i.e., approaching the lower bound of robustness). Towards this target, we propose a parameter-free Adaptive Auto Attack (A^3) evaluation method which addresses the efficiency and reliability in a test-time-training fashion. Specifically, by observing that adversarial examples to a specific defense model follow some regularities in their starting points, we design an Adaptive Direction Initialization strategy to speed up the evaluation. Furthermore, to approach the lower bound of robustness under the budget number of iterations, we propose an online statistics-based discarding strategy that automatically identifies and abandons hard-to-attack images. Extensive experiments demonstrate the effectiveness of our A^3 . Particularly, we apply A^3 to nearly 50 widely-used defense models. By consuming much fewer iterations than existing methods, i.e., 1/10 on average ($10\times$ speed up), we achieve lower robust accuracy in all cases. Notably, we won **first place** out of 1681 teams in CVPR 2021 White-box Adversarial Attacks on Defense Models competitions with this method. Code is available at: https://github.com/liuye6666/adaptive_auto_attack

1. Introduction

Despite the breakthroughs for a wide range of fields, deep neural networks (DNNs) [21, 23, 42, 52] have been shown high vulnerabilities to adversarial examples. For instance, inputs added with human-imperceptible perturbations can deceive DNNs to output unreasonable predictions [4, 11, 14–16, 30, 33, 50, 59, 60]. Meanwhile, various adversarial defense methods [9, 17, 18, 49] have been proposed to resist against malicious perturbations. Unfortunately, these defense methods could be broken by more advanced attack methods [7, 12, 44, 45], making it difficult to identify the state-of-the-art. Therefore, we urgently need a practical evaluation method to judge the adversarial robustness of different defense strategies.

Robustness evaluation can be defined as looking for defense models' lower bound of robustness given a budget number of iterations and a test dataset [7]. Under this task, in a white-box setting, the widely-used random sampling has been proven effective in generating diverse **starting points** for attacks in a large-scale study [7, 20, 31, 43]. In general, there are two kinds of random sampling strategies. From the perspective of input space, given an original image x of label y and a random perturbation ζ sampled from uniform distributions, the starting point is $x_{st} = x + \zeta$, e.g., Projected Gradient Descent (PGD) [31]. From the perspective of output space, given a classifier f and a randomly sampled direction of diversification w_d , evaluators generate starting points by maximizing the change of output, i.e., $w_d^T f(x)$. Intuitively, the random sampling strategy is sub-optimal since it is model-agnostic.

Comprehensive statistics on random sampling are conducted to verify if it is suboptimal. In other words, we want to study if adversarial examples to a specific defense model follow some regularities in their starting points. The statistic results on input space show that the adversarial examples' starting points are actually random. This is reasonable because the starting points are highly dependent on the corresponding input images, and the input images are randomly distributed in the high-dimensional space. However, the statistics results in the output space show that the direction of diversification to a specific defense model follows some regularities. Specifically, the direction of diversification is not evenly distributed but with a model-specific bias

*Corresponding author

in the positive/negative direction. Based on this observation, random sampling in the output space may not obtain a good starting point, slowing down robustness evaluation. To speed up the evaluation, we propose an Adaptive Direction Initialization (ADI) strategy in this paper. ADI firstly adopts an observer to record the direction of diversification of adversarial examples at the first restart. Then, based on these directions, ADI gives a novel way to generate better directions than random sampling for the following restarts.

Furthermore, we propose a novel iterative strategy to approach the lower bound of robustness with the budget number of iterations. Currently, a naïve iterative strategy that treats all images evenly and allocates them the same iterations is widely applied to robustness evaluation [6, 7, 20, 31, 32, 43, 51]. However, the naïve iterative strategy is questionable because it pays unnecessary efforts to perturb hard-to-attack images. Intuitively, given the budget number of iterations, the more examples we successfully attack, the closer robustness to the lower bound we obtain. Therefore, the number of iterations assigned to hard-to-attack images is a lower priority. Based on our observation that loss values can roughly reflect the difficulty of attacks, we propose an online statistics-based discarding strategy that automatically identifies and abandons hard-to-attack images. Specifically, we stop perturbing images with considerable difficulties at the beginning of every restart. For the remaining images, the same number of iterations are allocated to them. Obviously, the online statistics-based discarding strategy makes full use of the number of iterations and increases the chance of perturbing images to adversarial examples. We can further approach the lower bound of robustness based on this reliable strategy. Essentially, speeding up the evaluation is also closely related to improving the reliability because the saved iterations can be used to attack easy-to-attack examples, resulting in lower robust accuracy. By incorporating the above two strategies, a practical evaluation method Adaptive Auto Attack (A^3) is proposed in this paper.

To sum up, our main contributions are three-fold: 1) Based on comprehensive statistics, we propose an adaptive direction initialization (ADI) strategy which generates an adaptive direction than random sampling to speed up the robustness evaluation. 2) We propose an online statistics-based discarding strategy that automatically identifies and abandons hard-to-attack images to approach further the lower bound of robustness under the budget number of iterations. 3) Extensive experiments demonstrate the effectiveness and reliability of the method. Mainly, we apply A^3 to nearly 50 widely-used defense models, without parameters adjustment, our method achieves a lower robust accuracy and a faster evaluation. On average, by consuming 1/10 of the iterations state-of-the-arts used, our A^3 achieves the best robustness evaluation results.

2. Related Works

Many white-box attacks on defense models have been proposed for robustness evaluation. Fast Adaptive Boundary Attack (FAB) [6] aims at finding the minimal perturbation necessary to change the class of a given input. Projected Gradient Descent (PGD) [31] further improves the evaluation performance by assigning random perturbations as the starting point at every restart. Based on PGD, Goyal *et al.* [20] proposes a MultiTargeted attack (MT) that picks a new target class at each restart. Tashiro [43] provides a more effective initialization strategy to generate diverse starting points. Unfortunately, most of these promising methods overestimate the robustness [2, 12, 44, 45]. Potential reasons for this are improper hyper-parameters tuning and gradient masking [7]. Therefore, we urgently need a practical evaluation method that is convenient (*i.e.*, parameter-free), efficient (*i.e.*, less iterations), and reliable (*i.e.*, approaching the lower bound of robustness).

To address this issue, Croce *et al.* [7] proposed Auto Attack (AA) by integrating four attacks methods. Large-scale studies have shown that AA achieves lower robust test accuracy than existing methods. However, AA is inefficient since it requires a massive number of iterations for robustness evaluation. Instead of adopting an ensemble strategy, Yu *et al.* [51] harnessed latent features and introduced a unified ℓ_∞ -norm white-box attack algorithm LAFeAT to evaluate robustness more reliably. Yet, for all that, two disadvantages hamper LAFeAT in applying it to practical robustness evaluation. Firstly, the time and space complexity of LAFeAT are unacceptable since it needs to train new modules for each defense model using the training set. Secondly, LAFeAT is impracticable since training sets are often inaccessible in practical applications.

3. Methodology

3.1. Preliminaries

In this section, we give some background knowledge of adversarial attacks, as well as reviewing some white-box attacks on defense models. Given a C -class classifier: $f : \mathbf{x} \in [0, 1]^D \rightarrow \mathbb{R}^C$, where \mathbf{x} is the original image of label y , the model prediction is calculated by:

$$h(\mathbf{x}) = \operatorname{argmax}_{c=1, \dots, C} f_c(\mathbf{x}), \quad (1)$$

where $f_c(\mathbf{x})$ refers to the output logits of \mathbf{x} on the c -th class. The goal of untargeted adversarial attacks is fooling f to misclassify a human-imperceptible adversarial example $\mathbf{x}_{adv} = \mathbf{x} + \delta$, *i.e.*, $h(\mathbf{x}_{adv}) \neq y$. Different from untargeted attacks, targeted attacks aim at misleading f to classify \mathbf{x}_{adv} to a targeted label y_{tgt} , *i.e.*, $h(\mathbf{x}_{adv}) = y_{tgt}$. In this paper, we mainly focus on untargeted attacks. The

targeted version can be simply derived. By adopting ℓ_∞ distance to evaluate the imperceptibility of δ , *i.e.*, $\|\delta\|_\infty \leq \epsilon$, the constrained optimization problem is defined as:

$$\arg \max \mathcal{L}(f(x_{adv}), y) \quad s.t. \quad \|x_{adv} - x\|_\infty \leq \epsilon. \quad (2)$$

In the scenario of white-box adversarial attacks, attackers can access all information of the victims' model. One of the most popular methods is PGD [31]. Specifically, PGD calculates the gradient at iteration t step-by-step:

$$g^t = \nabla_{x_{adv}^t} \mathcal{L}(f(x_{adv}^t), y), \quad (3)$$

where x_{adv}^t is the adversarial example at iteration t and the starting point x_{st} is generated as:

$$x_{st} = x + \zeta, \quad (4)$$

where ζ is a random perturbation sampled from a uniform distribution $U(-\epsilon, \epsilon)^D$. Then, PGD generates an adversarial example by performing the iterative update:

$$x_{adv}^{t+1} = P_{x, \epsilon}(x_{adv}^t + \eta^t \cdot \text{sign}(g^t)), \quad (5)$$

where η^t is the step size at iteration t , x_{adv}^t is adversarial example at iteration t and $x_{adv}^0 = x_{st}$, function $P_{x, \epsilon}(\cdot)$ clips the input to the ϵ -ball of x . To accurately evaluate the robustness of defense models, PGD usually adopts multiple restarts. At each restart, the starting points are randomly sampled from the perturbation space.

To further improve the diversity of starting points, Tashiro *et al.* [43] propose ODI to find starting points by maximizing the change in the output space. To be specific, given a random direction of diversification w_d sampled from uniform distributions $U(-1, 1)^C$, ODI firstly calculates a normalized perturbation vector as follows:

$$v(x, f, w_d) = \frac{\nabla_x w_d^T f(x)}{\|\nabla_x w_d^T f(x)\|}, \quad (6)$$

and then generates starting points by maximizing the output change via the following iterative update:

$$\begin{aligned} x_{adv}^{t+1} &= x_{adv}^t + \eta_{odi} \cdot \text{sign}(v(x_{adv}^t, f, w_d)), \\ x_{adv}^{t+1} &= P_{x, \epsilon}(x_{adv}^{t+1}), \end{aligned} \quad (7)$$

where η_{odi} is the step size for initialization and x_{adv}^0 is calculated by Eq. (4). After N_{odi} iterations, *i.e.*, number of iteration for initialization, ODI obtains the starting point x_{st} :

$$x_{st} = x_{adv}^{N_{odi}}. \quad (8)$$

As same as PGD, ODI performs multiple restarts to achieve lower robust accuracy.

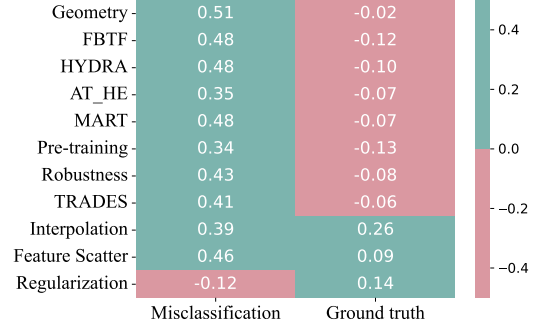


Figure 1. Quantitative statistical results of the direction of diversification w_d of adversarial examples on 11 models. The direction w_d for all models disobey a uniform distribution.

3.2. Motivations

A practical evaluation method should be convenient (*i.e.*, parameter-free¹), efficient (*i.e.*, fewer iterations), and reliable (*i.e.*, approaching the lower bound of robustness). Although using a large number of iterations, most of the existing methods usually overestimate the robustness. There are two potential reasons for this: a) Despite the effectiveness of generating diverse starting points for attacks, random sampling is suboptimal since they are model-agnostic. Exploiting random sampling to generate starting points will slow the robustness evaluation down, and b) The widely adopted naïve iterative strategy, *i.e.*, treating all examples evenly and allocating them the same iterations, is questionable. Intuitively, naïve iterative strategy pays unnecessary efforts to perturb hard-to-attack images.

To verify the above two points, we conduct a comprehensive statistic analysis on some methods of white-box adversarial attacks against defense models. Next, we provide a detailed analysis.

Random sampling is suboptimal. Considering Eq. (8) and Eq. (4), random sampling is widely used to generate diverse starting points for attacks in the input space (*e.g.*, PGD), and output space (*e.g.*, ODI). It is worth noting that there is no need to do statistics on random sampling in the input space, since the starting points are highly dependent on the corresponding input images and the input images are randomly distributed in the high-dimensional space of the input space. Therefore, we mainly focus on random sampling in the output space.

As shown in Eq. (7), the noise in the output space is determined by w_d . Therefore, to verify the unreasonableness of random sampling in the output space, we analyze w_d of adversarial examples (*i.e.*, examples that were successfully attacked) and explore what kind of w_d is conducive. Specifically, we adopt ODI parameterized by number of restarts $R = 50$, $N_{odi} = 7$ and $\eta_{odi} = \epsilon$. The number of iterations

¹Following [7], 'parameter-free' indicates that we do not need the fine-tuning of parameters for every new defense.

for attacks at each restarts N_{atk} is set to 30, and the step size at t -th iteration is formulated as follows:

$$\eta^t = \frac{1}{2}\epsilon \cdot \left(1 + \cos \left(\frac{t \bmod N_{atk}}{N_{atk}} \pi \right) \right). \quad (9)$$

Then we use ODI to attack 11 defense models, including Geometry [58], FBTF [47], HYDRA [39], AT-HE [35], MART [46], Pre-training [22], Robustness [13], TRADES [56], Interpolation [55], Feature Scatter [54], Regularization [25]. Among adversarial examples against different models, we summarize statistic results of w_d in Fig. 1. The 1st and 2nd columns give mean values of w_d at the \hat{y} -th (the misclassification label), i.e., $\overline{w_d^{\hat{y}}}$, and the y -th (the ground truth), i.e., $\overline{w_d^y}$.

From Fig. 1, we have the following observations. Firstly, the direction of diversification w_d disobeys uniform distribution. Secondly, the direction of diversification with model-specific bias in the positive/negative direction. Mainly, there are three kinds of biases: **a)** $\overline{w_d^y} < 0$, $\overline{w_d^{\hat{y}}} > 0$, **b)** $\overline{w_d^y} > 0$, $\overline{w_d^{\hat{y}}} > 0$, and **c)** $\overline{w_d^y} > 0$, $\overline{w_d^{\hat{y}}} < 0$. Considering Eq. (7), for **a**, $f_y(x_{st})$, $f_{\hat{y}}(x_{st})$ are decreased and increased, respectively, which satisfies the goal of adversarial attacks. For **b**, both of $f_y(x_{st})$ and $f_{\hat{y}}(x_{st})$ are increased. For **c**, $f_y(x_{st})$ is increased and $f_{\hat{y}}(x_{st})$ is decreased. Obviously, cases **b** and **c** are counter-intuitive, a potential reason is that these defense models adopt gradient masks [34]. Based on these observations, random sampling is suboptimal since it is model-agnostic. Adopting it to generate starting points hinders the algorithms from approaching the lower bound of robustness rapidly.

Limitations of Naïve iterative strategy. Most of the existing methods adopt the naïve iterative strategy, i.e., treats all images evenly. However, based on two intuitions: (1) Images vary in difficulty to perturb them to adversarial examples, and (2) The higher the difficulty, the more iterations are needed to perturb them. Naïve iterative strategy is impractical because it pays unnecessary efforts to perturb hard-to-attack images. In order to successfully attack more images and get closer to the lower bound of robustness with the budget number of iterations, the number of iterations assigned to hard-to-attack images is a lower priority. Therefore, we need a method that can roughly reflect the hard-to-attack images and easy-to-attack images to allocate the budget number of iterations reasonably.

Intuitively, the loss function values can roughly reflect the difficulty of perturbing an image to an adversarial example. Multiple loss functions $\mathcal{L}(\cdot)$ can be used for attacks, including the cross-entropy loss and the margin loss defined as $\max_{c \neq y} f_c(x) - f_y(x)$. In this paper, we use the margin loss and define hard-to-attack images as images that cannot be successfully attacked even after 2000 iterations. The other images that are successfully attacked, we define as easy-to-attack images.

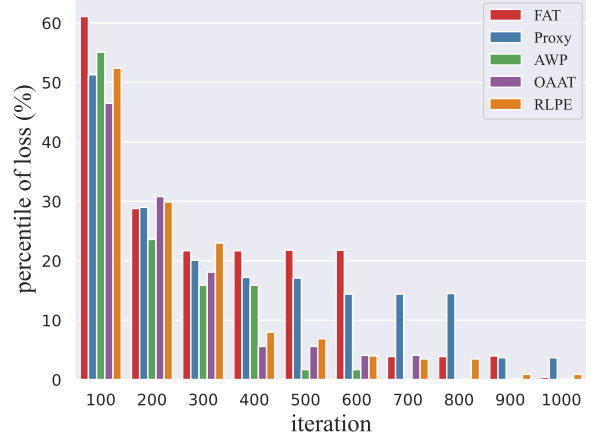


Figure 2. Quantitative statistical results of loss percentile of easy-to-attack images. As the number of iterations increases, the loss ranking of easy-to-attack images get higher and higher.

To verify that loss values can distinguish between hard-to-attack and easy-to-attack images, we first perform 2000 attacks with ODI on all images of 5 models (including, AWP [48], FAT [57], Proxy [38], OAAT [1], RLPE [41]), and then identify and mark the easy-to-attack images of each model. Finally, we attack the 5 models again with ODI to record the percentile of loss values in descending order for easy-to-attack images in the process of attacks. We visualized the statistical results in Fig. 2.

From this figure, we have the following observations. For all models, the loss percentiles of easy-to-attack images continually decrease as the number of iterations increases, indicating that easy-to-attack images are getting higher and higher in loss ranking, accordingly, more and more images with low loss ranking are hard-to-attack images. In other words, the distinction between hard-to-attack and easy-to-attack images becomes more and more accurate. We can roughly distinguish between hard-to-attack and easy-to-attack images according to the loss values. Based on these observations, to make full use of the budget number of iterations, we can automatically abandon hard-to-attack images with an increasing proportion during the process of attacks.

3.3. Adaptive Direction Initialization

Inspired by the above analysis of random sampling in Sec. 3.2, we propose a method named Adaptive Direction Initialization (ADI) to generate better directions than random sampling to initialize the attacks. Specifically, ADI has two steps: *useful directions observer* and *adaptive directions generation*.

For *useful directions observer* step, ADI first adopts the random sampling to generate the direction of diversification, i.e., $w_d = U(-1, 1)^C$. Then ADI uses the starting points obtained by Eq. (8) to initialize PGD attacks and obtains adversarial examples crafted by PGD. We denote W

as a set containing w_d of all adversarial examples.

Motivated by Sec. 3.2, for *adaptive directions generation*, ADI adopts the sign of the summed w_d in W as prior knowledge to generate the adaptive direction w_a :

$$\kappa_c(W) = \text{sign}\left(\sum_{w_d \in W} w_d^c\right), \quad (10)$$

where $\kappa_c(W)$ is the prior knowledge of generating w_a^c , i.e., the c -th dimension of w_a . With the help of $\kappa(\cdot)$, ADI generates the y -th components of w_a as:

$$w_a^y = \begin{cases} w_a^y \sim U(-0.5, 0.1), & \kappa_y(\cdot) < 0, \\ w_a^y \sim U(-0.1, 0.5), & \kappa_y(\cdot) > 0. \end{cases} \quad (11)$$

To improve the effectiveness of w_a , ADI randomly selects a label η to follow the sign of symbol of $\kappa_\eta(\cdot)$:

$$w_a^\eta = \begin{cases} -0.8, & \kappa_\eta(\cdot) < 0, \\ 0.8, & \kappa_\eta(\cdot) > 0. \end{cases} \quad (12)$$

Notably, our method is insensitive to w_a^η experimentally. For simplicity, we set $w_a^\eta = \pm 0.8$. For the remaining dimensions of adaptive direction w_a , ADI calculates them as:

$$w_a^i \sim U(-1, 1)^{C-2}, i = \text{other}. \quad (13)$$

Compared with random sampling adopted by ODI, the adaptive direction generated by ADI is guided by prior knowledge, i.e., the direction of diversification of adversarial examples. Furthermore, ADI randomly generates the remaining $C - 2$ dimensions of the adaptive direction to improve the diversity of starting points.

3.4. Online Statistics-based Discarding Strategy

In light of approaching the lower bound of robustness with the budget number of iterations, we propose a novel iterative strategy named Online Statistics-based Discarding (OSD). According to the observation in Sec. 3.2, OSD adopts loss values to distinguish between hard-to-attack images and easy-to-attack images. OSD first sorts the images in descending order by the corresponding loss values at the beginning of every restart. Then it discards, i.e., stopping perturbing images with small loss values. Particularly, given an initial discarding rate ϕ and an discarding increment ι , the discarding rate at the r -th restart is formulated as follows:

$$\varsigma^r = \phi + r \times \iota. \quad (14)$$

For the remaining images, OSD assigns the same number of iterations to them. Intuitively, to further increase the attack success rate, OSD allocates more iterations to remaining images at restart r than the previous restart. Concretely, given an initial number of iteration γ for attacks and an iteration increment ν , the number of iterations for attacks at the r -th restart is computed as follows:

$$N_{atk}^r = \gamma + r \times \nu. \quad (15)$$

Algorithm 1: Adaptive Auto Attack (A^3)

Inputs: norm bound ϵ , the number of iteration for initialization N , step sizes η , the number of iteration for attacks at the r -th restart N_{atk}^r , attack iteration step sizes η_{atk} , number of restarts R , test dataset \mathcal{I}

Outputs: Adversarial example x_{adv}^{t+1}

for $r = 0 \rightarrow R$ **do**

 Update the test dataset \mathcal{I} by OSD

for x in \mathcal{I} **do**

 Sample ζ from $U(-\epsilon, \epsilon)^D$

$x_{st} = x + \zeta$

if $r = 0$ **then**

 Sample w_d from $U(-1, 1)^C$

else

$w_d \leftarrow w_a$

 /* ADI */

for $n = 0$ to N **do**

 Compute x_{adv}^{n+1} by Eq. (7)

for $t = 0$ to N_{atk}^r **do**

 Compute x_{adv}^{t+1} by Eq. (5)

if $r=0$ **then**

 Compute w_a by Eqs. (11) to (13).

if x_{adv}^{t+1} is an adversarial example **then**

return x_{adv}^{t+1}

Compared with naïve iterative strategy, OSD makes full use of the budget number of iterations by automatically identifying and abandoning hard-to-attack images. In addition, by allocating various number of iterations for attacks at different restarts, OSD helps to further approach the lower bound of adversarial robustness.

3.5. Adaptive Auto Attack

We integrate the above two strategies to form a practical evaluation method Adaptive Auto Attack (A^3). Firstly, A^3 is convenient since we do not need the fine-tuning of parameters for every new defense models. Secondly, A^3 is efficient. For the gradient-based optimization to craft adversarial examples, unlike random sampling, our method A^3 generates adaptive directions for each model and provides better starting points to speed up the evaluation. Thirdly, A^3 is reliable. By discarding hard-to-attack images online and adjusting iterations for attacks adaptively, our method A^3 makes full use of a budget number of iterations and further approaches the lower bound of adversarial robustness. Compared with the mainstream method AA, our parameter-free A^3 is a more efficient and reliable protocol for robustness evaluation. We hope that A^3 will serve as a benchmark for evaluating the robustness of various deep models and defense methods. The algorithm of Adaptive Auto Attack is summarized in Algorithm 1.

4. Experiments

We conduct comprehensive experiments to evaluate the practicability of our method. Specifically, five baselines are included: PGD [31], ODI [43], MT-PGD [20], I-FGSM [29] and AA [7]. Nearly 50 ℓ_∞ -defense models with 8 different architectures are chosen from recent conferences like ICML, NeurIPS, ICLR, ICCV, CVPR. To be specific, the evaluation is performed on 35 and 12 defense models trained on CIFAR-10 and CIFAR-100 [27] datasets, respectively. Notably, for fair comparisons, the step size is calculated by Eq. (9) for all attack methods in the experiments. We use the margin loss for all attack methods.

Following AA, we adopt robust accuracy (**acc**) in this paper to reflect evaluation reliability. A robustness evaluation method is considered reliable if it can significantly downgrade the model’s classification accuracy. Furthermore, we assume a similar computational complexity among all methods in each iteration. So the evaluation efficiency of each method can be directly reflected by the total number of iterations. In our experiments, for AA and A^3 , we compute the evaluation efficiency of both forward propagation (“ \rightarrow ”) and backward propagation (“ \leftarrow ”).

4.1. Comparisons with State-of-the-Art Attacks

To comprehensively validate the efficiency and reliability of our method, we evaluate the attack performance and efficiency of AA, PGD, ODI, and our A^3 on nearly 50 defense models. The evaluation results are shown in Tab. 1.

Setup. Following the setup of ODI and PGD, 100 iterations are allocated for each image (4 restarts, 25 iterations for attacks at each restart), and $N = 2$. For AA, the standard version² is adopted. For our method A^3 , the initial number of iterations for attacking γ is set to 25, and the iteration increment ν is 5. When it reaches 50, we keep it unchanged to save the budget number of iterations. The initial discarding rate $\phi = 0$ and the discarding increment $\iota = 0.1$, when the discarding rate reaches to 0.9, we gradually increase it to 0.97 at an interval of $\iota = 0.035$.

Results. As can be seen in Tab. 1, A^3 uses the same parameters for all defense models and achieves lower robust accuracies than AA in all cases, downgrading **acc** by 0.1% on average. Besides, our method achieves a faster evaluation, on average, 10.4 \times speed up for forward propagation, and 5.4 \times for backward propagation. In general, the nature of parameter-free, reliability, and efficiency enables A^3 to be a practical method for robustness evaluation.

4.2. Ablation Study

Efficacy of adaptive direction initialization. To evaluate the effectiveness of ADI, we design another variant called Reverse Adaptive Direction Initialization (R-ADI) which

adopts the reverse direction of the adaptive direction. For all methods, we allocate 150 iterations for each image (5 restarts and 30 iterations at each restart.), and $N=10$.

The comparison results among R-ADI, ODI, and ADI are reported in Tab. 2. As can be seen, compared to ODI, our ADI achieves better attack performance in all cases. The result indicates the initial direction does affect the performance. Compared with uniformly generating initial direction, our proposed ADI can generate the model-specific initial direction and help to obtain better performance. In general, R-ADI achieves the worst performance in all cases. One possible reason is that R-ADI chooses a bad initial direction, which hinders the performance.

Efficacy of online statistics-based discarding strategy.

To verify the effect of OSD, we compare the robust accuracy curves of the defense models under the attack of ADI, ADI+OSD (A^3), and AA. For our methods ADI and ADI+OSD, the setup is the same as in Sec. 4.1.

Note that ADI+OSD denotes the Online Statistics-based Discarding strategy is applied on ADI. The result is shown in the Fig. 3. As can be observed, it costs more iterations for AA to achieve the same robust accuracy of ADI and ADI+OSD in all cases. Meanwhile, in order to achieve higher attack performance, the number of iterations of ADI and AA significantly increases, but our ADI+OSD ascends gently. The curves reveal the efficiency of our ADI+OSD, especially for reliable attacks.

Efficacy on other robustness evaluation methods. In this section, we study the effect of integrating ADI and OSD into different robustness evaluation methods. For all methods, we allocate 500 iterations for each image (5 restarts and 100 iterations for attacks at each restart), and $N=10$. For MT-PGD, the number of multiple targets is 3. For our method A^3 , the initial number of iterations for attacking γ is set to 25, and the iteration increment ν is 5. When it reaches 50, we keep it unchanged to save the budget number of iterations. The initial discarding rate $\phi = 0$ and the discarding increment $\iota = 0.2$, when the discarding rate reaches to 0.9, we gradually increase it to 0.97 at an interval of $\iota = 0.035$.

Tab. 3 shows the robust accuracy (%) of defense models under the attack of different attack methods [20, 29, 31, 43] integrated with our modules (ADI and OSD). It shows that ADI and OSD can be integrated into multiple attack methods and effectively improve their performance.

4.3. Result of Competition

With our proposed A^3 , we participated in track 1 of the CVPR 2021 Security AI Challenger Competition. In track 1, they required competitors to perform white-box adversarial attacks on ML defense models. The competition has three stages. Stage 1 and stage 2 employed 13 and 2 defense models trained on CIFAR-10 and ImageNet datasets, respectively. Images for attacks contain the first 1,000

²<https://github.com/fra31/auto-attack>

| CIFAR-10 Defense Method | Model | Clean | Nominal | PGD | ODI | AA | | | A ³ | | | Δ |
|---------------------------------|-------------|-------|---------|-------|-------|-------|-------|-------|---------------------|--------------|-------------|----------|
| | | acc | acc | acc | acc | acc | → | ← | acc | → | ← | acc |
| ULAT [19] [†] | WRN-70-16 | 91.10 | 65.87 | 66.75 | 66.06 | 65.88 | 51.20 | 12.90 | 65.78 ↓ 0.10 | 4.49(11.40×) | 2.20(5.86×) | ↓ 0.09 |
| Fixing Data [36] | WRN-70-16 | 88.54 | 64.20 | 65.10 | 64.46 | 64.25 | 50.82 | 12.59 | 64.19 ↓ 0.06 | 4.41(11.52×) | 2.17(5.81×) | ↓ 0.01 |
| ULAT [19] [†] | WRN-28-10 | 89.48 | 62.76 | 63.63 | 63.01 | 62.80 | 49.62 | 12.30 | 62.70 ↓ 0.10 | 4.28(11.58×) | 2.10(5.85×) | ↓ 0.05 |
| Fixing Data [36] | WRN-28-10 | 87.33 | 60.73 | 61.64 | 61.09 | 60.75 | 47.98 | 11.91 | 60.66 ↓ 0.09 | 4.14(11.59×) | 2.04(5.83×) | ↓ 0.07 |
| RLPE [41] [†] | WRN-34-15 | 86.53 | 60.41 | 61.25 | 60.69 | 60.41 | 47.53 | 11.82 | 60.31 ↓ 0.10 | 4.12(11.52×) | 2.02(5.84×) | ↓ 0.10 |
| AWP [48] [†] | WRN-28-10 | 88.25 | 60.04 | 60.55 | 60.23 | 60.04 | 47.20 | 11.70 | 59.98 ↓ 0.06 | 4.09(11.54×) | 2.01(5.82×) | ↓ 0.06 |
| RLPE [41] [†] | WRN-28-10 | 89.46 | 59.66 | 60.78 | 59.88 | 59.66 | 47.09 | 11.72 | 59.51 ↓ 0.15 | 4.10(11.49×) | 2.00(5.85×) | ↓ 0.15 |
| Geometry [58] ^{†‡} | WRN-28-10 | 89.36 | 59.64 | 60.17 | 59.59 | 59.64 | 47.10 | 11.67 | 59.53 ↓ 0.11 | 4.10(11.49×) | 2.00(5.85×) | ↓ 0.11 |
| RST [5] [†] | WRN-28-10 | 89.69 | 62.50 | 60.64 | 59.44 | 59.53 | 47.10 | 11.70 | 59.42 ↓ 0.11 | 4.10(11.49×) | 2.01(5.82×) | ↓ 3.08 |
| Proxy [38] [†] | WRN-34-10 | 85.85 | 59.09 | 60.51 | 59.94 | 59.09 | 46.70 | 11.60 | 58.99 ↓ 0.10 | 4.04(11.56×) | 1.98(5.86×) | ↓ 0.10 |
| OAAT [1] | WRN-34-10 | 85.32 | 58.04 | 58.84 | 58.25 | 58.04 | 45.64 | 11.34 | 57.98 ↓ 0.06 | 3.99(11.43×) | 1.96(5.76×) | ↓ 0.06 |
| HYDRA [39] [†] | WRN-28-10 | 88.98 | 59.98 | 58.27 | 57.60 | 57.14 | 45.20 | 11.20 | 57.06 ↓ 0.08 | 3.91(11.56×) | 1.92(5.83×) | ↓ 2.92 |
| ULAT [19] | WRN-70-16 | 85.29 | 57.20 | 57.90 | 57.48 | 57.20 | 45.20 | 11.20 | 57.08 ↓ 0.12 | 3.90(11.59×) | 1.92(5.83×) | ↓ 0.12 |
| ULAT [19] | WRN-34-20 | 85.64 | 56.82 | 57.40 | 57.00 | 56.86 | 44.96 | 11.18 | 56.76 ↓ 0.10 | 3.88(11.60×) | 1.90(5.89×) | ↓ 0.10 |
| MART [46] [†] | WRN-28-10 | 87.50 | 65.04 | 58.09 | 56.80 | 56.29 | 44.60 | 11.10 | 56.20 ↓ 0.09 | 3.86(11.55×) | 1.89(5.93×) | ↓ 8.84 |
| Pre-training [22] [†] | WRN-34-10 | 87.11 | 57.40 | 56.43 | 55.32 | 54.92 | 43.40 | 10.80 | 54.76 ↓ 0.16 | 3.73(11.64×) | 1.83(5.90×) | ↓ 2.64 |
| Proxy [38] | ResNet-18 | 84.38 | 55.60 | 56.31 | 54.98 | 54.43 | 43.21 | 10.71 | 54.35 ↓ 0.08 | 3.75(11.52×) | 1.84(5.81×) | ↓ 1.25 |
| AT_HE [35] | WRN-34-20 | 85.14 | 62.14 | 55.33 | 54.21 | 53.74 | 43.00 | 10.69 | 53.67 ↓ 0.07 | 3.68(11.68×) | 1.81(5.91×) | ↓ 8.47 |
| LBGAT [8] [‡] | WRN-34-20 | 88.70 | 53.57 | 54.69 | 53.90 | 53.57 | 43.11 | 10.58 | 53.46 ↓ 0.11 | 3.69(11.63×) | 1.81(5.80×) | ↓ 0.11 |
| FAT [57] | WRN-34-10 | 84.52 | 53.51 | 54.46 | 53.83 | 53.51 | 42.94 | 10.54 | 53.42 ↓ 0.09 | 3.68(11.72×) | 1.81(5.83×) | ↓ 0.09 |
| Overfitting [37] | WRN-34-20 | 85.34 | 58.00 | 55.21 | 53.95 | 53.42 | 42.10 | 10.50 | 53.33 ↓ 0.09 | 3.66(11.50×) | 1.80(5.83×) | ↓ 4.67 |
| Self-adaptive [24] [‡] | WRN-34-10 | 83.48 | 58.03 | 54.39 | 53.62 | 53.33 | 42.10 | 10.50 | 53.20 ↓ 0.13 | 3.66(11.50×) | 1.80(5.83×) | ↓ 4.83 |
| TRADES [56] [‡] | WRN-34-10 | 84.92 | 56.43 | 54.02 | 53.31 | 53.08 | 42.00 | 10.40 | 53.01 ↓ 0.07 | 3.63(11.57×) | 1.78(5.75×) | ↓ 3.42 |
| LBGAT [8] [‡] | WRN-34-10 | 88.22 | 52.86 | 54.37 | 53.26 | 52.86 | 41.80 | 10.30 | 52.76 ↓ 0.10 | 3.64(11.48×) | 1.79(5.79×) | ↓ 0.10 |
| OAAT [1] | ResNet-18 | 80.24 | 51.06 | 51.69 | 51.28 | 51.06 | 40.54 | 10.21 | 51.02 ↓ 0.04 | 3.51(11.53×) | 1.72(5.93×) | ↓ 0.04 |
| SAT [40] | WRN-34-10 | 86.84 | 50.72 | 52.95 | 51.38 | 50.72 | 40.14 | 10.01 | 50.62 ↓ 0.10 | 3.50(11.46×) | 1.72(5.81×) | ↓ 0.10 |
| Robustness [13] | ResNet-50 | 87.03 | 53.29 | 52.19 | 50.14 | 49.21 | 39.10 | 9.80 | 49.16 ↓ 0.05 | 3.42(11.43×) | 1.68(5.83×) | ↓ 4.13 |
| YOPO [53] | WRN-34-10 | 87.20 | 47.98 | 47.11 | 45.57 | 44.83 | 35.60 | 9.00 | 44.77 ↓ 0.06 | 3.09(11.52×) | 1.52(5.92×) | ↓ 3.21 |
| MMA [10] | WRN-28-4 | 84.36 | 47.18 | 47.78 | 42.42 | 41.51 | 33.30 | 8.60 | 41.27 ↓ 0.24 | 3.17(11.50×) | 1.66(5.19×) | ↓ 5.85 |
| DNR [28] | ResNet-18 | 87.32 | 40.41 | 42.15 | 41.01 | 40.41 | 32.81 | 8.72 | 40.26 ↓ 0.15 | 2.81(11.67×) | 1.38(6.32×) | ↓ 5.93 |
| CNL [3] [‡] | ResNet-18 | 81.30 | 79.67 | 40.26 | 40.23 | 40.22 | 32.70 | 8.70 | 39.83 ↓ 0.39 | 2.74(11.93×) | 1.34(6.49×) | ↓ 39.84 |
| Feature Scatter [54] | WRN-28-10 | 89.98 | 60.60 | 54.63 | 42.91 | 36.62 | 30.00 | 8.20 | 36.31 ↓ 0.33 | 11.02(2.72×) | 5.44(1.51×) | ↓ 24.33 |
| Interpolation [55] | WRN-28-10 | 90.25 | 68.70 | 66.72 | 49.35 | 36.45 | 30.00 | 8.50 | 36.21 ↓ 0.24 | 11.21(2.64×) | 5.52(1.54×) | ↓ 32.32 |
| Sensible [26] | WRN-34-10 | 91.51 | 57.23 | 56.04 | 43.15 | 34.22 | 28.20 | 7.80 | 34.00 ↓ 0.22 | 10.66(2.65×) | 5.25(1.49×) | ↓ 23.23 |
| Regularization [25] | ResNet-18 | 90.84 | 77.68 | 52.77 | 19.73 | 1.35 | 3.10 | 2.30 | 0.89 ↓ 0.46 | 2.24(1.38×) | 1.09(2.11×) | ↓ 76.79 |
| <hr/> | | | | | | | | | | | | |
| CIFAR-100 Defense Method | Model | Clean | Nominal | PGD | ODI | AA | | | A ³ | | | Δ |
| | | acc | acc | acc | acc | acc | → | ← | acc | → | ← | acc |
| ULAT [19] [†] | WRN-70-16 | 69.15 | 36.88 | 38.64 | 37.41 | 36.88 | 29.84 | 7.42 | 36.86 ↓ 0.02 | 2.56(11.64×) | 1.25(5.92×) | ↓ 0.02 |
| Fixing Data [36] | WRN-70-16 | 63.56 | 34.64 | 35.95 | 34.98 | 34.64 | 28.02 | 6.96 | 34.55 ↓ 0.09 | 2.38(11.76×) | 1.16(6.00×) | ↓ 0.04 |
| Fixing Data [36] | WRN-28-10 | 62.41 | 32.06 | 33.39 | 32.36 | 32.06 | 25.53 | 6.48 | 32.00 ↓ 0.06 | 2.24(11.38×) | 1.10(5.90×) | ↓ 0.06 |
| OAAT [1] | WRN-34-10 | 65.73 | 30.35 | 31.62 | 30.93 | 30.35 | 24.34 | 6.11 | 30.31 ↓ 0.04 | 2.18(11.14×) | 1.07(5.70×) | ↓ 0.04 |
| LBGAT [8] [‡] | WRN-34-20 | 62.55 | 30.20 | 31.65 | 30.49 | 30.20 | 23.97 | 6.10 | 30.12 ↓ 0.08 | 2.16(11.11×) | 1.05(5.80×) | ↓ 0.08 |
| ULAT [19] | WRN-70-16 | 60.86 | 30.03 | 31.03 | 30.41 | 30.03 | 23.93 | 6.09 | 29.99 ↓ 0.04 | 2.13(11.23×) | 1.04(5.86×) | ↓ 0.04 |
| LBGAT [8] [‡] | WRN-34-10 | 60.64 | 29.33 | 30.56 | 29.63 | 29.33 | 23.21 | 5.94 | 29.18 ↓ 0.15 | 2.11(11.00×) | 1.03(5.77×) | ↓ 0.15 |
| AWP [48] | WRN-34-10 | 60.38 | 28.86 | 30.70 | 29.45 | 28.86 | 23.01 | 5.84 | 28.78 ↓ 0.08 | 2.10(10.96×) | 1.02(5.72×) | ↓ 0.08 |
| Pre-training [22] | WRN-28-10 | 59.23 | 28.42 | 30.56 | 29.13 | 28.42 | 22.74 | 5.73 | 28.31 ↓ 0.11 | 2.08(10.93×) | 1.02(5.61×) | ↓ 0.11 |
| OAAT [1] | ResNet18 | 62.02 | 27.14 | 27.90 | 27.47 | 27.14 | 21.74 | 5.61 | 27.09 ↓ 0.05 | 2.34(9.29×) | 1.15(4.88×) | ↓ 0.05 |
| SAT [40] | WRN-34-10 | 62.82 | 24.57 | 26.69 | 25.43 | 24.57 | 19.70 | 5.10 | 24.51 ↓ 0.06 | 1.90(10.36×) | 0.93(5.48×) | ↓ 0.06 |
| Overfitting [37] | PAResNet-18 | 53.83 | 18.95 | 20.15 | 19.39 | 18.95 | 15.28 | 4.00 | 18.90 ↓ 0.05 | 1.64(9.32×) | 0.80(5.00×) | ↓ 0.05 |

Table 1. Comparison of robust accuracy (%) under the attack of A³ against PGD, ODI, and AutoAttack(AA) across various defense strategies. The “acc” column shows the robust accuracies of different models. The “Nominal” column shows the robust accuracies reported by defense models. The “ Δ ” column shows the difference between the robust accuracies of “Nominal” and A³. The “→” column shows the iteration number of forward propagation (million), while the “←” column shows the iteration number of backward propagation (million). Models marked with [†] were additionally trained with unlabeled datasets. We used $\epsilon = 8/255$ except for models marked with [‡], which used $\epsilon = 0.031$ as originally reported by the authors. Notably, the “acc” column of A³ shows the difference between the robust accuracies of AA and A³, the “←” and “→” columns of A³ show the speedup factors of A³ relative to AA.

images from the CIFAR-10 test set and randomly chosen 1,000 images from ILSVRC 2012 validation set. Finally, attack methods tested on all test sets of CIFAR-10 dataset and 1,000 random images of the ImageNet validation set

to evaluate the final score. The evaluation score is defined as the average misclassification rate. Finally, we obtained 51.10% score in the final stage and achieved first place among 1681 teams.

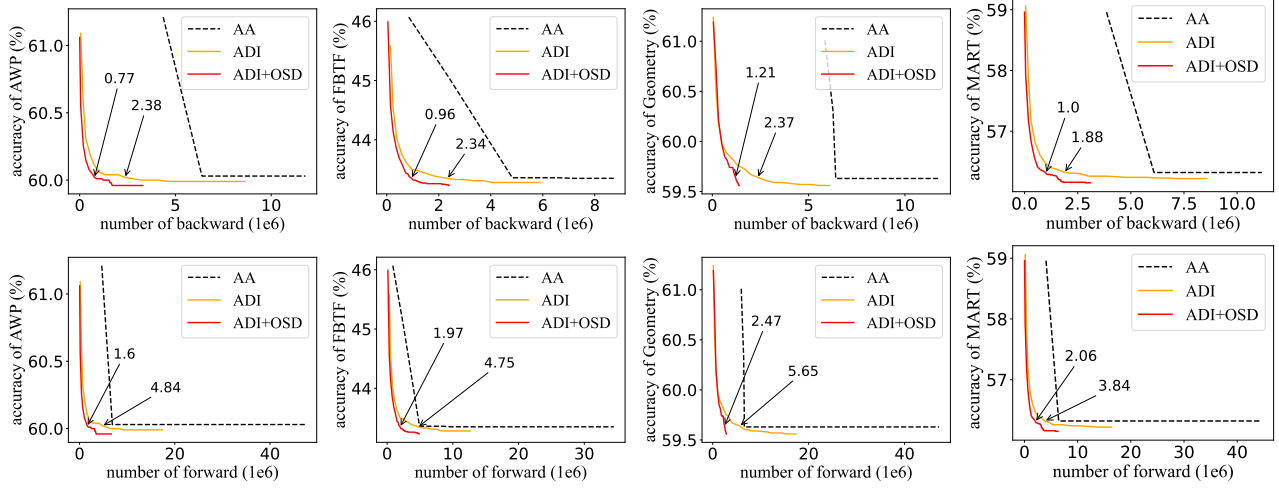


Figure 3. Comparisons of performance of ADI+OSD, ADI and AA on 4 defenders. For each defender, we separately record the number of forward propagation and back propagation by columns. The horizontal axes show the number of back propagation (top) and forward propagation (bottom). The vertical axes show the percentage of remaining unsuccessful examples. The iteration numbers needed for ADI+OSD and ADI to defeat AA are also marked.

| Defense method | R-ADI | ODI | ADI |
|-----------------|------------------------|-------|--------------------------------|
| Geometry | 60.00 \uparrow 0.09 | 59.91 | 59.73 \downarrow 0.18 |
| RST | 59.81 \uparrow 0.01 | 59.80 | 59.63 \downarrow 0.17 |
| Proxy | 59.65 \uparrow 0.25 | 59.40 | 59.22 \downarrow 0.18 |
| HYDRA | 57.47 \uparrow 0.11 | 57.36 | 57.26 \downarrow 0.10 |
| MART | 56.86 \uparrow 0.28 | 56.58 | 56.48 \downarrow 0.10 |
| Pre-training | 55.48 \uparrow 0.37 | 55.11 | 54.96 \downarrow 0.15 |
| Self-adaptive | 53.59 \uparrow 0.11 | 53.48 | 53.33 \downarrow 0.15 |
| Feature Scatter | 40.90 \uparrow 2.22 | 38.68 | 38.29 \downarrow 0.39 |
| Interpolation | 55.47 \uparrow 12.95 | 42.52 | 40.01 \downarrow 2.51 |
| Sensible | 41.14 \uparrow 3.19 | 37.95 | 37.19 \downarrow 0.76 |
| Regularization | 24.82 \uparrow 14.83 | 9.99 | 7.75 \downarrow 2.24 |

Table 2. Comparisons of robust accuracy (%) under attack of ADI, naïve ODI and R-ADI across various defense strategies. R-ADI obtains the worst results because it chose the worst starting points.

5. Conclusion

In this paper, we find that model-agnostic initial directions drawn from uniform distributions result in unsatisfactory robust accuracy, and naïve iterative strategy leads to unreliable attacks. We propose a novel approach called Adaptive Auto Attack (A^3) to address these issues, which adopts adaptive direction initialization and an online statistics-based discarding strategy to achieve efficient and reliable robustness evaluation. Extensive experiments demonstrate the effectiveness of A^3 . Particularly, we achieve lower robust accuracy in all cases by consuming much fewer iterations than existing models, *e.g.*, 1/10 on average (10 \times speed up). We won first place out of 1,681 teams in CVPR 2021 White-box Adversarial Attacks on Defense Models competitions with this method.

| Attack method | PoE-robustness | Self-adaptive | OAAT | Feature scatter |
|-----------------|---------------------------------------|---------------------------------------|---------------------------------------|--|
| I-FGSM | 60.77 | 54.38 | 51.74 | 55.00 |
| I-FGSM+ADI | 59.66 \downarrow 1.12 | 53.36 \downarrow 1.02 | 51.09 \downarrow 0.65 | 38.24 \downarrow 16.76 |
| I-FGSM+ADI+OSD | 59.50 \downarrow 1.28 | 53.24 \downarrow 1.14 | 51.01 \downarrow 0.73 | 36.70 \downarrow 18.30 |
| PGD | 60.65 | 54.29 | 51.5 | 52.98 |
| PGD+ADI | 59.61 \downarrow 1.04 | 53.37 \downarrow 0.92 | 51.08 \downarrow 0.42 | 38.08 \downarrow 14.90 |
| PGD+ADI+OSD | 59.51 \downarrow 1.14 | 53.23 \downarrow 1.06 | 51.04 \downarrow 0.46 | 36.72 \downarrow 16.26 |
| MT-PGD | 60.51 | 54.08 | 51.59 | 50.92 |
| MT-PGD+ADI | 60.11 \downarrow 0.40 | 53.69 \downarrow 0.39 | 51.50 \downarrow 0.09 | 38.41 \downarrow 12.51 |
| MT-PGD+ADI+OSD | 59.71 \downarrow 0.80 | 53.34 \downarrow 0.74 | 51.18 \downarrow 0.41 | 36.74 \downarrow 14.18 |
| ODI-PGD | 59.74 | 53.49 | 51.13 | 38.56 |
| ODI-PGD+ADI | 59.65 \downarrow 0.09 | 53.34 \downarrow 0.15 | 51.09 \downarrow 0.04 | 37.92 \downarrow 0.64 |
| ODI-PGD+ADI+OSD | 59.51 \downarrow 0.23 | 53.26 \downarrow 0.23 | 51.00 \downarrow 0.13 | 36.75 \downarrow 1.17 |

Table 3. Effectiveness of the two modules ADI and OSD on 4 different attack methods.

6. Broader Impacts

Performing reliable robustness evaluation has a substantial potential impact since it helps distinguish good from bad defenses to resist against the widespread adversarial examples. Our research proposes a parameter-free, efficient, and reliable robustness evaluation method, revealing the possibility of performing a practical evaluation. On the positive side, our method enables us to identify advanced defenses to defend against adaptive attacks, preventing critical safety systems from crashing. On the negative side, malicious users can exploit our method to attack the system, raising a security risk. Finally, while this method achieves state-of-the-art robust test accuracy, this is not an exhaustive survey. We will continue to expand the scope of our evaluation for advanced defenses in the future.

Acknowledgements

We thank the Security AI Challenger program launched by Alibaba Group and Tsinghua University.

References

- [1] Sravanti Addepalli, Samyak Jain, Gaurang Sriramanan, Shivangi Khare, and Venkatesh Babu Radhakrishnan. Towards achieving adversarial robustness beyond perceptual limits. In *ICML 2021 Workshop on Adversarial Machine Learning*, 2021. 4, 7
- [2] Anish Athalye, Nicholas Carlini, and David Wagner. Obfuscated gradients give a false sense of security: Circumventing defenses to adversarial examples. In *ICML*, 2018. 2
- [3] Matan Atzmon, Niv Haim, Lior Yariv, Ofer Israelov, Haggai Maron, and Yaron Lipman. Controlling neural level sets. In *NeurIPS*, pages 2032–2041, 2019. 7
- [4] Nicholas Carlini and David A. Wagner. Towards evaluating the robustness of neural networks. In *SP*, 2017. 1
- [5] Yair Carmon, Aditi Raghunathan, Ludwig Schmidt, John C. Duchi, and Percy Liang. Unlabeled data improves adversarial robustness. In *NeurIPS*, pages 11190–11201, 2019. 7
- [6] Francesco Croce and Matthias Hein. Minimally distorted adversarial examples with a fast adaptive boundary attack. In *ICML*, 2020. 2
- [7] Francesco Croce and Matthias Hein. Reliable evaluation of adversarial robustness with an ensemble of diverse parameter-free attacks. In *ICML*, pages 2206–2216. PMLR, 2020. 1, 2, 3, 6
- [8] Jiequan Cui, Shu Liu, Liwei Wang, and Jiaya Jia. Learnable boundary guided adversarial training. In *ICCV*, pages 15721–15730, October 2021. 7
- [9] Guneet S. Dhillon, Kamyar Azizzadenesheli, Zachary C. Lipton, Jeremy Bernstein, Jean Kossaifi, Aran Khanna, and Animashree Anandkumar. Stochastic activation pruning for robust adversarial defense. In *ICLR*, 2018. 1
- [10] Gavin Weiguang Ding, Yash Sharma, Kry Yik Chau Lui, and Ruitong Huang. MMA training: Direct input space margin maximization through adversarial training. In *ICLR. Open-Review.net*, 2020. 7
- [11] Yinpeng Dong, Fangzhou Liao, Tianyu Pang, Hang Su, Jun Zhu, Xiaolin Hu, and Jianguo Li. Boosting adversarial attacks with momentum. In *CVPR*, pages 9185–9193, 2018. 1
- [12] Yinpeng Dong, Tianyu Pang, Hang Su, and Jun Zhu. Evading defenses to transferable adversarial examples by translation-invariant attacks. In *CVPR*, 2019. 1, 2
- [13] Logan Engstrom, Andrew Ilyas, Hadi Salman, Shibani Santurkar, and Dimitris Tsipras. Robustness (python library), 2019. 4, 7
- [14] Lianli Gao, Yaya Cheng, Qilong Zhang, Xing Xu, and Jingkuan Song. Feature space targeted attacks by statistic alignment. In *IJCAI*, 2021. 1
- [15] Lianli Gao, Qilong Zhang, Jingkuan Song, Xianglong Liu, and Heng Tao Shen. Patch-wise attack for fooling deep neural network. In *ECCV*, 2020. 1
- [16] Lianli Gao, Qilong Zhang, Jingkuan Song, and Heng Tao Shen. Patch-wise++ perturbation for adversarial targeted attacks. *CoRR*, abs/2012.15503, 2020. 1
- [17] Zhitao Gong, Wenlu Wang, and Wei-Shinn Ku. Adversarial and clean data are not twins. *arXiv preprint arXiv:1704.04960*, 2017. 1
- [18] Ian J. Goodfellow, Jonathon Shlens, and Christian Szegedy. Explaining and harnessing adversarial examples. In *ICLR*, 2015. 1
- [19] Sven Gowal, Chongli Qin, Jonathan Uesato, Timothy A. Mann, and Pushmeet Kohli. Uncovering the limits of adversarial training against norm-bounded adversarial examples. *CoRR*, abs/2010.03593, 2020. 7
- [20] Sven Gowal, Jonathan Uesato, Chongli Qin, Po-Sen Huang, Timothy A. Mann, and Pushmeet Kohli. An alternative surrogate loss for pgd-based adversarial testing. *arXiv preprint arXiv:1910.09338*, 2019. 1, 2, 6
- [21] Kaiming He, Xiangyu Zhang, Shaoqing Ren, and Jian Sun. Deep residual learning for image recognition. In *CVPR*, pages 770–778, 2016. 1
- [22] Dan Hendrycks, Kimin Lee, and Mantas Mazeika. Using pre-training can improve model robustness and uncertainty. In *ICML*, volume 97 of *Proceedings of Machine Learning Research*, pages 2712–2721. PMLR, 2019. 4, 7
- [23] Gao Huang, Zhuang Liu, Laurens van der Maaten, and Kilian Q. Weinberger. Densely connected convolutional networks. In *CVPR*, 2017. 1
- [24] Lang Huang, Chao Zhang, and Hongyang Zhang. Self-adaptive training: beyond empirical risk minimization. In *NeurIPS*, 2020. 7
- [25] Charles Jin and Martin Rinard. Manifold regularization for adversarial robustness. *CoRR*, abs/2003.04286, 2020. 4, 7
- [26] Jungeum Kim and Xiao Wang. Sensible adversarial learning. 2019. 7
- [27] Alex Krizhevsky, Geoffrey Hinton, et al. Learning multiple layers of features from tiny images. 2009. 6
- [28] Souvik Kundu, Mahdi Nazemi, Peter A. Beerel, and Masoud Pedram. DNR: A tunable robust pruning framework through dynamic network rewiring of dnns. In *ASPDAC*, pages 344–350. ACM, 2021. 7
- [29] Alexey Kurakin, Ian J. Goodfellow, and Samy Bengio. Adversarial examples in the physical world. In *ICLR Workshop*, pages 99–112, 2017. 6
- [30] Jiadong Lin, Chuanbiao Song, Kun He, Liwei Wang, and John E. Hopcroft. Nesterov accelerated gradient and scale invariance for adversarial attacks. In *ICLR*, 2020. 1
- [31] Aleksander Madry, Aleksandar Makelov, Ludwig Schmidt, Dimitris Tsipras, and Adrian Vladu. Towards deep learning models resistant to adversarial attacks. In *ICLR. OpenReview.net*, 2018. 1, 2, 3, 6
- [32] Xiaofeng Mao, Yuefeng Chen, Shuhui Wang, Hang Su, Yuan He, and Hui Xue. Composite adversarial attacks. In *AAAI*. 2
- [33] Seyed-Mohsen Moosavi-Dezfooli, Alhussein Fawzi, and Pascal Frossard. Deepfool: A simple and accurate method to fool deep neural networks. In *CVPR*, 2016. 1
- [34] Linh Nguyen, Sky Wang, and Arunesh Sinha. A learning and masking approach to secure learning. In *GameSec*, 2018. 4
- [35] Tianyu Pang, Xiao Yang, Yinpeng Dong, Taufik Xu, Jun Zhu, and Hang Su. Boosting adversarial training with hypersphere embedding. In *NeurIPS*, 2020. 4, 7
- [36] Sylvestre-Alvise Rebuffi, Sven Gowal, Dan A. Calian, Florian Stimberg, Olivia Wiles, and Timothy A. Mann. Fixing data augmentation to improve adversarial robustness. *CoRR*, abs/2103.01946, 2021. 7

- [37] Leslie Rice, Eric Wong, and J. Zico Kolter. Overfitting in adversarially robust deep learning. In *ICML*, volume 119 of *Proceedings of Machine Learning Research*, pages 8093–8104. PMLR, 2020. 7
- [38] Vikash Sehwal, Saeed Mahloujifar, Tinashe Handina, Sihui Dai, Chong Xiang, Mung Chiang, and Prateek Mittal. Improving adversarial robustness using proxy distributions. *CoRR*, abs/2104.09425, 2021. 4, 7
- [39] Vikash Sehwal, Shiqi Wang, Prateek Mittal, and Suman Jana. HYDRA: pruning adversarially robust neural networks. In *NeurIPS*, 2020. 4, 7
- [40] Chawin Sitawarin, Supriyo Chakraborty, and David A. Wagner. Improving adversarial robustness through progressive hardening. *CoRR*, abs/2003.09347, 2020. 7
- [41] Kaustubh Sridhar, Oleg Sokolsky, Insup Lee, and James Weimer. Robust learning via persistency of excitation. *CoRR*, abs/2106.02078, 2021. 4, 7
- [42] Christian Szegedy, Vincent Vanhoucke, Sergey Ioffe, Jonathon Shlens, and Zbigniew Wojna. Rethinking the inception architecture for computer vision. In *CVPR*, 2016. 1
- [43] Yusuke Tashiro, Yang Song, and Stefano Ermon. Diversity can be transferred: Output diversification for white- and black-box attacks. *arXiv preprint arXiv:2003.06878*, 2020. 1, 2, 3, 6
- [44] Florian Tramer, Nicholas Carlini, Wieland Brendel, and Aleksander Madry. On adaptive attacks to adversarial example defenses. In *NeurIPS*, 2020. 1, 2
- [45] Jonathan Uesato, Brendan O’donoghue, Pushmeet Kohli, and Aaron Oord. Adversarial risk and the dangers of evaluating against weak attacks. In *ICML*, 2018. 1, 2
- [46] Yisen Wang, Difan Zou, Jinfeng Yi, James Bailey, Xingjun Ma, and Quanquan Gu. Improving adversarial robustness requires revisiting misclassified examples. In *ICLR*. OpenReview.net, 2020. 4, 7
- [47] Eric Wong, Leslie Rice, and J. Zico Kolter. Fast is better than free: Revisiting adversarial training. In *ICLR*, 2020. 4
- [48] Dongxian Wu, Shu-Tao Xia, and Yisen Wang. Adversarial weight perturbation helps robust generalization. In *NeurIPS*, 2020. 4, 7
- [49] Cihang Xie, Jianyu Wang, Zhishuai Zhang, Zhou Ren, and Alan L. Yuille. Mitigating adversarial effects through randomization. In *ICLR*, 2018. 1
- [50] Cihang Xie, Zhishuai Zhang, Yuyin Zhou, Song Bai, Jianyu Wang, Zhou Ren, and Alan L. Yuille. Improving transferability of adversarial examples with input diversity. In *CVPR*, pages 2730–2739, 2019. 1
- [51] Yunrui Yu, Xitong Gao, and Cheng-Zhong Xu. Lafeat: Piercing through adversarial defenses with latent features. In *CVPR*, 2021. 2
- [52] Sergey Zagoruyko and Nikos Komodakis. Wide residual networks. *arXiv preprint arXiv:1605.07146*, 2016. 1
- [53] Dinghui Zhang, Tianyuan Zhang, Yiping Lu, Zhanxing Zhu, and Bin Dong. You only propagate once: Accelerating adversarial training via maximal principle. In *NeurIPS*, pages 227–238, 2019. 7
- [54] Haichao Zhang and Jianyu Wang. Defense against adversarial attacks using feature scattering-based adversarial training. In *NeurIPS*, pages 1829–1839, 2019. 4, 7
- [55] Haichao Zhang and Wei Xu. Adversarial interpolation training: A simple approach for improving model robustness. 2019. 4, 7
- [56] Hongyang Zhang, Yaodong Yu, Jiantao Jiao, Eric P. Xing, Laurent El Ghaoui, and Michael I. Jordan. Theoretically principled trade-off between robustness and accuracy. In *ICML*, volume 97 of *Proceedings of Machine Learning Research*, pages 7472–7482. PMLR, 2019. 4, 7
- [57] Jinfeng Zhang, Xilie Xu, Bo Han, Gang Niu, Lizhen Cui, Masashi Sugiyama, and Mohan S. Kankanhalli. Attacks which do not kill training make adversarial learning stronger. In *ICML*, volume 119 of *Proceedings of Machine Learning Research*, pages 11278–11287. PMLR, 2020. 4, 7
- [58] Jinfeng Zhang, Jianing Zhu, Gang Niu, Bo Han, Masashi Sugiyama, and Mohan S. Kankanhalli. Geometry-aware instance-reweighted adversarial training. In *ICLR*. OpenReview.net, 2021. 4, 7
- [59] Qilong Zhang, Xiaodan Li, Yuefeng Chen, Jingkuan Song, Lianli Gao, Yuan He, and Hui Xue. Beyond imagenet attack: Towards crafting adversarial examples for black-box domains. In *ICLR*, 2022. 1
- [60] Zhengyu Zhao, Zhuoran Liu, and Martha A. Larson. Towards large yet imperceptible adversarial image perturbations with perceptual color distance. In *CVPR*, 2020. 1